Electronic Supplementary Information

Construction of ternary $RuP_2/Ti_4P_6O_{23}@TiO_2$ photocatalyst for efficient photocatalytic biomass selective oxidation and water splitting

Xinze Li[a#], Qiong Liu[b#], Jiliang Ma[a,c*], Kangning Liu[a], Zhendong Liu[a], and Runcang Sun[a*]

[a] Liaoning Key Lab of Lignocellulose Chemistry and BioMaterials, Liaoning Collaborative Innovation Center for Lignocellulosic Biorefinery, College of Light Industry and Chemical Engineering, Dalian Polytechnic University, Dalian 116034, China

[b] Institute of Analysis, Guangdong Academy of Sciences (China National Analytical Center, Guangzhou), Guangzhou, Guangdong, 510070, China

[c] Guangxi Key Laboratory of Clean Pulp & Papermaking and Pollution Control. College of Light Industrial and Food Engineering, Guangxi University, Nanning 530004, China

*Corresponding authors' E-mail address**:** jlma@dlpu.edu.cn (Jiliang Ma) and rcsun3@dlpu.edu.cn (Runcang Sun), Tel.: +86-0411-86323652, Fax: +86-0411-86323652

Chemicals

Tryptophan (Trp, 99.0%), potassium iodide (KI, 99.0%), benzoquinone (BQ, 99.0%), isopropyl (IPA, 99.0%), rhamnose (98.0%), xylose (98.0%), xylan (85.0%), arabinose (98.0%), mannose (98.0%), fructose (98.0%), glucose (98.0%), potassium hydroxide (KOH, 99.0%), and nano titanium dioxide (TiO_2, 99.8%) were acquired from Aladdin Chemistry Co., Ltd (Shanghai, China). Sodium hypophosphite (NaH_2PO_2, 98.0%) and ruthenium trichloride ($RuCl_3$, 45.0 ~ 55.0%) were obtained from Macklin biochemical Co., Ltd (Shanghai, China). Chloroplatinic acid hexahydrate ($H_2PtCl_6 \cdot 6H_2O$, ≥ 37.5% Pt basis), lactic acid (99.0%), formic acid (99.0%), and other chemicals were purchased from Dalian Chemical Reagent Factory, China.

Characterization

Transmission electron microscopy (TEM) were recorded on JEM-2100 CXII and scanning electron microscopy (SEM) were explored on Hitachis-4800. The powder X-ray diffraction (XRD) patterns were measured with a Bruker D8 Focus diffractometer (CuKα radiation, λ = 0.15418 nm) in the θ-2θ mode. Brunauer-Emmett-Teller (BET) specific surface areas were measured on a Micromeritics ASAP 2020 apparatus. The X-ray photoelectron spectroscopy (XPS) analysis was performed with a Kratos Axis Ultra DLD spectrometer employing an amonochromated AlKR X-ray source (1486.6 eV). The ultraviolet-visible diffuse reflectance spectrum (UV-vis DRS) was achieved on a Cary 5000 spectrophotometer by using $BaSO_4$ as the reference. The photoluminescence (PL) spectrum was measured by an Edinburgh

FLS-920 spectrometer. Electron spin-resonance spectroscopy was used to study molecules and materials with unpaired electrons, and the 5,5-dimethyl-1-pyrroline N-oxide (DMPO) was chosen as a spin trap for the detection of hydroxyl radical (·OH) and superoxide ($\cdot O_2^-$), the 2,2,6,6-tetramethylpiperidine-1-oxyl (TEMPO) was applied to characterize electrons and holes, while the amino-2,2,6,6-tetramethylpiperidine (TEMPONE) was used to detect singlet oxygen. Ultraviolet photoelectron spectroscopy (UPS) was measured by using a He I (21.20 eV) as monochromatic discharge light source and a VG Scienta R4000 analyzer. A sample bias of -5 V was applied to observe the secondary electron cutoff (SEC).

Photoelectrochemical Measurements

Electrochemical measurements were carried out on a CHI760E electrochemical workstation with a stand three-electrodes system. Among them, a Pt wire was used as the counter electrode, and the reference electrode was the saturated Ag/AgCl. The cleaned F-doped tin oxide (FTO) glass was used as the working electrode. 5 mg of corresponding photocatalyst and 20 μL of Nafion (5%) were added into 980 μL of ethanol to form a homogeneous slurry. The homogeneous slurry was ultrasonicated for 30 min and then coated on the FTO glass. The obtained system was dried at 150 ^oC for 60 min. The supporting electrolyte was Na_2SO_4 solution (0.5 M) with the pH value of 6.8. The incident visible light source was Xe lamp (300 W). The photocurrent-time was investigated in the irradiation of Xe lamp at a bias potential of 0.5 V vs. Ag/AgCl. The electrochemical impedance spectroscopy (EIS) was detected by an AC voltage amplitude of 10 mV at -0.3 V versus Ag/AgCl over the frequency

range from 10 kHz to 0.01 Hz. The Mott-Schottky was studied in the electrolyte of Na_2SO_4 (0.5 M), and the frequency of the AC potential was set as 500, 800, and 1000 Hz as well as the amplitude was 10 mV.

Products Analysis

The photocatalytic performance was measured with the Perfectlight PCX 50C multi-channel photochemical reaction system under the illumination of 10 W LED lamps.

Hydrogen:

The yield of hydrogen was analyzed by gas chromatography (GC-7900, Ar carrier gas, molecular sieve 5 Å column) equipped with a thermal conductivity detector (TCD).

Products of Oxidation Half-reaction:

After the reaction, the samples were filtrated with a Millipore filter (0.22 μm) and analyzed by high-performance liquid chromatography (HPLC) with a Bio-Rad Aminex HPX-87H column (300 mm × 7.8 mm × 9 μm). Concentrations of lactic acid was measured by Waters 2414 RI detector. The mobile phase was 5 mmol H_2SO_4 at a flow rate of 0.5 mL/min. The temperature of column was set at 55 ^oC and the total time to finish the product analysis was set at 30 min. The conversion and yields of oxidation half-reaction products were calculated as follows:

$$Conversion\ (\%) = \frac{Moles\ of\ carbon\ in\ feedstock\ consumed}{Moles\ of\ carbon\ in\ feedstock\ input} \times 100\%$$

$$Product\ yield\ (\%) = \frac{Moles\ of\ carbon\ in\ organic\ acid}{Moles\ of\ carbon\ in\ feedstock\ input} \times 100\%$$

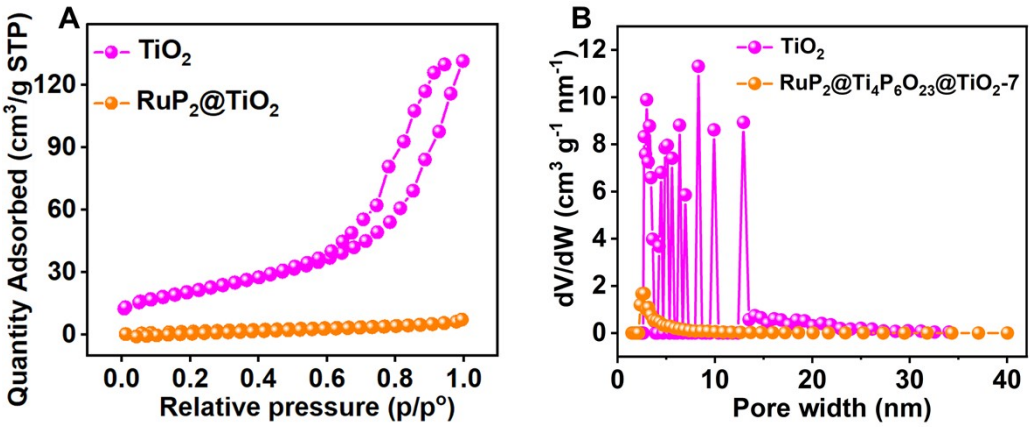

Fig. S1 N_2 adsorption-desorption isotherm of TiO_2 and $RuP_2/Ti_4P_6O_{23}@TiO_2$-7 (A). Pore width distribution of TiO_2 and $RuP_2/Ti_4P_6O_{23}@TiO_2$-7 (B).

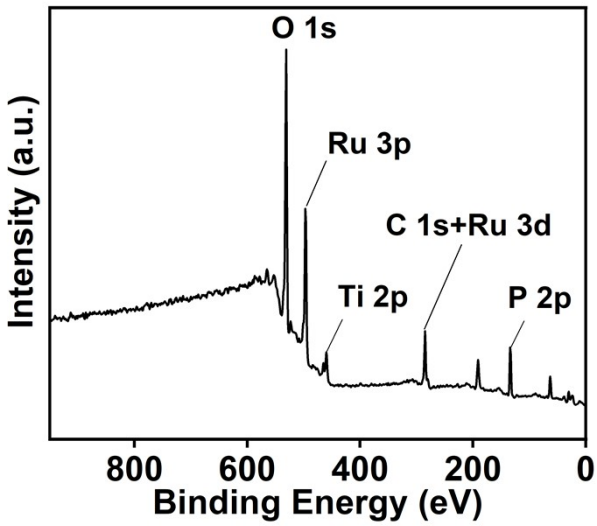

Fig. S2 XPS survey spectra of $RuP_2/Ti_4P_6O_{23}@TiO_2$-7.

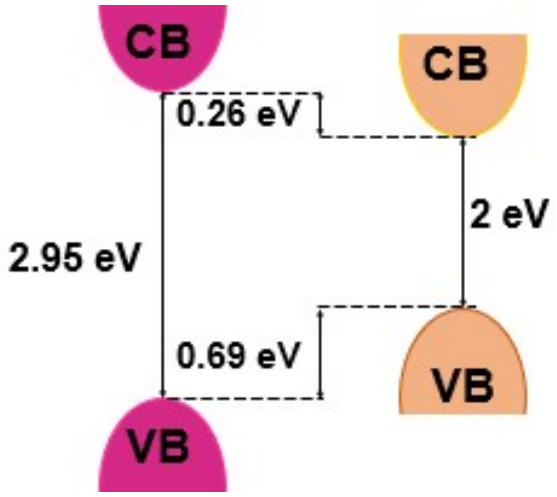

Fig. S3 Relative band alignment of TiO_2 and $RuP_2/Ti_4P_6O_{23}@TiO_2$-7.

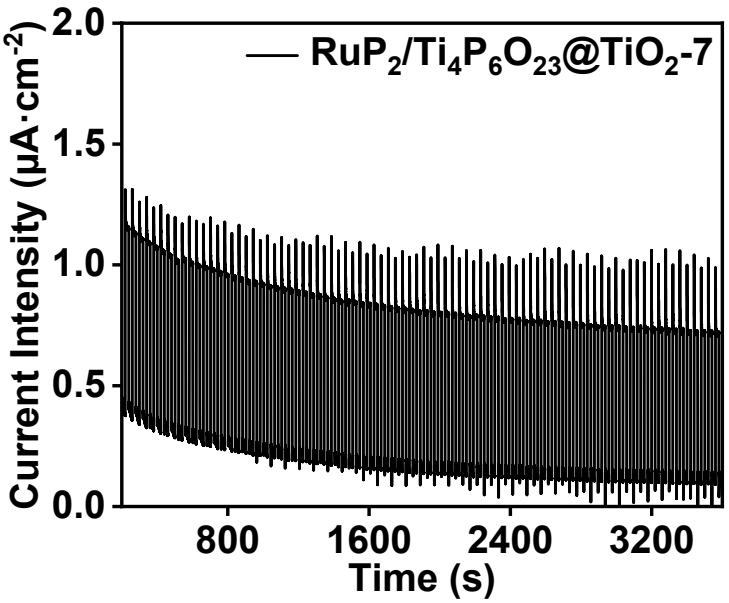

Fig. S4 Long-term transient photocurrent response of $RuP_2/Ti_4P_6O_{23}@TiO_2$-7.

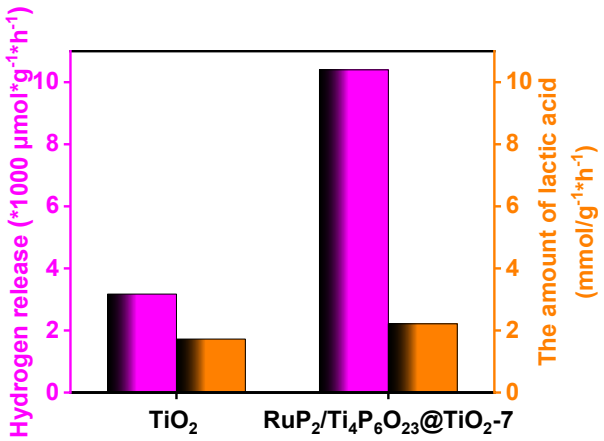

Fig. S5 The effects of RuP_2 on the photocatalytic synchronous biorefinery and hydrogen evolution.

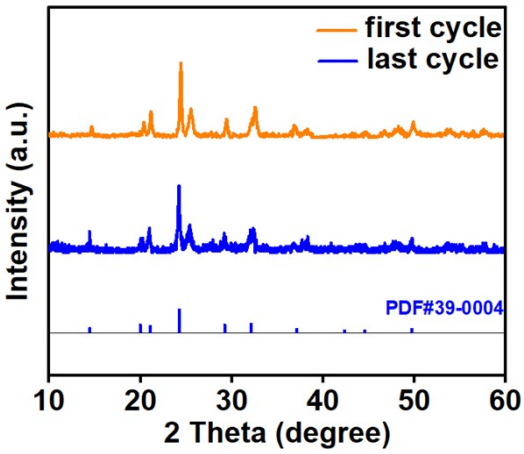

Fig. S6 The first cycle and last cycle XRD of $RuP_2/Ti_4P_6O_{23}@TiO_2$-7

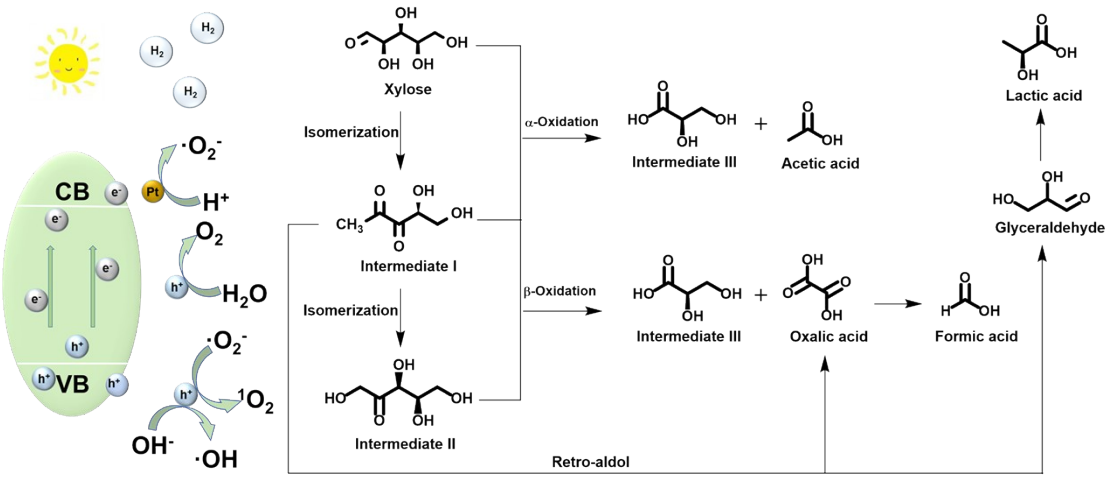

Fig. S7 The possible reaction pathway of co-production of hydrogen and lactic acid from xylose over $RuP_2/Ti_4P_6O_{23}@TiO_2$-7.

Table S1. The effects of different TiO_2-based materials on the hydrogen evolution

Photocatalysis	Reaction conditions	Hydrogen evolution ($\mu mol\ g^{-1}\ h^{-1}$)	Ref.
$RuP_2/Ti_4P_6O_{23}@TiO_2$-7 [a]	Xylose (5 mg/ml), Visible-light	16269.2	This work
WO_3/TiO_2/rGO [b]	methanol, = 365 nm	245.8	[1]
TiO_2/ZnS-5 [c]	TAOH, Visible-light	5503.8	[2]
Co_2P/TiO_2 [d]	methanol, Visible-light	409.5	[3]
(CCT) Carbon dots/g-C_3N_4/TiO_2 [e]	Triethanolamine, > 420 nm	580.0	[4]
$CdS/Ag/TiO_2$ [f]	Na_2S solution, > 420 nm	806.3	[5]

Reaction conditions: [a] 30.0 °C, 6 h; [b] 50 mg, 3 h; [c] 3 h; [d] 4 h; [e] 50 mg, 3 h; [f] 3.5 h;

References

1 F. He, A. Meng, B. Cheng, W. Ho and J. Yu, *Chinese J. Catal.,* 2020, **41**, 9-20.

2 Q. Wang, G. Wang, J. Wang, J. Li, K. Wang, S. Zhou and Y. Su, *Adv. Sustain. Syst.,* 2022, **11**, 2200027.

3 W. Ding, X. Zhang, Q. Wang, X. Jiang, L. Xiao and H. Du, *Energy Technol-ger.,* 2022, **10**, 2200059.

4 Z. Hu, D. Shi, G. Wang, T. Gao, J. Wang, L. Lu and J. Li, *Appl. Surf. Sci.,* 2022, **601**, 154167.

5 X. Xu, T. Wang, M. Xu, X. Yang, J. Hou, D. Cao and Q. Wang, *Spectrochim. Acta A.,* 2022, **276**, 121215.